HEFAT2007
5th International Conference on Heat Transfer, Fluid Mechanics and Thermodynamics
1-4 July 2007, Sun City, South Africa
Paper number: CM3

BUOYANCY-INDUCED HEAT TRANSFER FROM AN INCLINED TUBE-ARRAY

C. Cianfrini, M. Corcione* and E. Habib
*Author for correspondence
Dipartimento di Fisica Tecnica, University of Rome "La Sapienza"
via Eudossiana, 18 – 00184 Rome, Italy
e-mail: massimo.corcione@uniroma1.it

ABSTRACT

Steady laminar free convection in air from an inclined array of parallel circular cylinders, is studied numerically. SIMPLE-C algorithm is used for the solution of the mass, momentum, and energy transfer governing equations. Simulations are performed for tube-arrays consisting of 3 to 7 cylinders equally-spaced at a center-to-center separation distance of 2 cylinder-diameters, tilting angles from 0° to 90° (which correspond to the vertical and horizontal settings, respectively), and Rayleigh numbers in the range between 10^2 and 10^6. It is found that the thermal performance of the whole array increases (a) with increasing both the Rayleigh number and the tilting angle, and (b) as the number of cylinders either decreases at small inclinations or increases at large inclinations.

INTRODUCTION

Buoyancy-induced heat transfer from inclined tube-arrays has received a small degree of attention, despite the numerous possible engineering applications, e.g., heat exchangers, just to cite one.

In fact, besides a first experimental work conducted by Liebermann and Gebhart [1], who investigated the thermal behavior of an array of ten widely-spaced long wires at a very low Grashof number, only another paper on this topic was readily found in the literature. However, this study, which was performed experimentally by Sparrow and Boessneck [2], is related to a simple two-cylinder geometry, and to a narrow range of the Rayleigh number.

In this background, the aim of the present paper is to investigate free convection in air from a tube-array inclined with respect to the gravity vector, with the main objective to highlight the main effects of the tilting angle on the flow and temperature fields, and on the amount of heat exchanged by any individual element of the array and by the whole tube-assembly. The study is conducted numerically under the assumption of isothermal surfaces, and two-dimensional steady laminar flow. Simulations are performed for tube-arrays consisting of 3 to 7 circular cylinders equally-spaced at an assigned center-to-center separation distance of 2 cylinder-diameters, inclination angles of the array in the range between 0° and 90°, which correspond to the vertical and horizontal configurations, respectively, and Rayleigh numbers in the range between 10^2 and 10^6.

PROBLEM FORMULATION

A tube-array consisting of N horizontal circular cylinders set parallel to one another in a plane inclined of an angle φ with respect to the gravity vector, is considered. The diameter D of the cylinders, and their centre-to-centre separation distance S, are assigned. Free convection heat transfer occurs between each cylinder surface, kept at uniform temperature t_w, and the surrounding undisturbed fluid reservoir, assumed at uniform temperature t_∞.

The buoyancy-induced flow is considered to be steady, two-dimensional, and laminar. The fluid is assumed incompressible, with constant physical properties and negligible viscous dissipation and pressure work. Buoyancy effects on momentum transfer are taken into account through the Boussinesq approximation.

Governing equations

Once the above assumptions are employed in the conservation equations of mass, momentum, and energy, the following set of dimensionless governing equations is obtained:

$$\nabla \cdot \mathbf{V} = 0 \tag{1}$$

$$(\mathbf{V}\cdot\nabla)\mathbf{V} = -\nabla p + \nabla^2 \mathbf{V} - \frac{Ra}{Pr} T \frac{\mathbf{g}}{g} \tag{2}$$

$$(\mathbf{V}\cdot\nabla)T = \frac{1}{Pr}\nabla^2 T \tag{3}$$

where $\mathbf{V}$ is the velocity vector having dimensionless velocity components (U,V) normalized with (ν/D), T is the dimensionless temperature excess over the uniform temperature of the undisturbed fluid reservoir normalized with the temperature

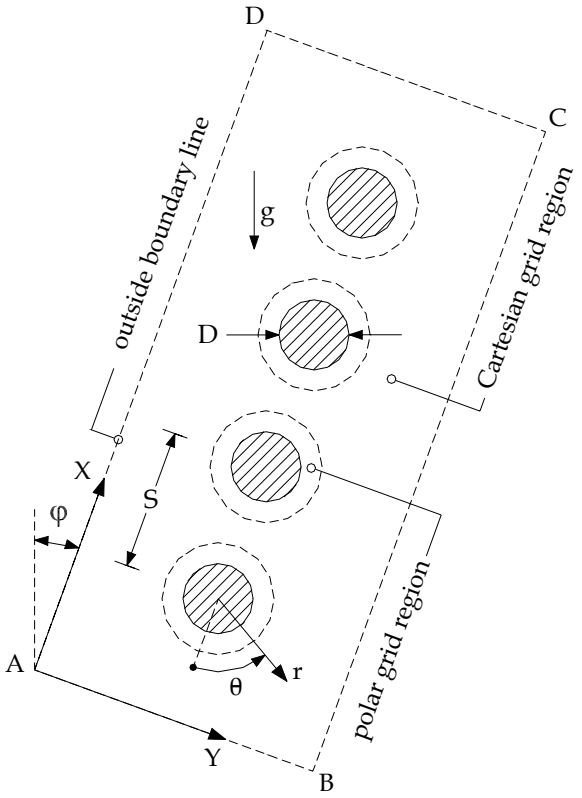

Figure 1 – Geometry, coordinate systems and integration domain

difference ($t_w - t_\infty$), p is the dimensionless pressure normalized with ($\rho_\infty v^2/D^2$), Ra is the Rayleigh number based on the cylinder-diameter, **g** is the gravity vector, and Pr is the Prandtl number.

The related boundary conditions are T = 1 and **V** = 0 at any cylinder surface, and T = 0 and **V** = 0 at very large distance from the cylinders.

Computational domain and discretization grid system

The finite-difference solution of equations (1)–(3) with the boundary conditions stated above requires that a discretization grid system is established across the whole two-dimensional integration domain, which is taken as a rectangle which includes all the cylinders and extends sufficiently far from them. A cylindrical polar grid is employed in the proximity of any cylinder, while a Cartesian grid is used to fill the remainder of the integration domain, as sketched in Fig. 1, where the (r, θ) and (X, Y) coordinate systems adopted are also represented. In the polar systems, U is the radial velocity component, and V is the tangential velocity component. In the Cartesian system, whose origin is taken at the bottom left corner of the integration domain, U and V are the X-wise and Y-wise components of the velocity vector, respectively. According to the discretization scheme originally proposed by Launder and Massey [3], the cylindrical polar grids and the Cartesian grid, which are entirely independent of one another, overlap with no attempt of node-matching. Their connection is provided by two sets of false nodes, one for each neighboring grid, located beyond their intersection, as described in more details in a recent paper by Corcione [4].

Boundary conditions

The boundary conditions required for the numerical solution of the governing equations (1)–(3) have to be specified at any cylinder surface, and at the four boundary lines which enclose the two-dimensional integration domain defined above. In particular, once such boundary lines are placed sufficiently far from the cylinders, the motion of the fluid entering or leaving the computational domain may reasonably be assumed to occur normally to them. The entering fluid is assumed at the undisturbed free field temperature. As regards the leaving fluid, whose temperature is unknown, a zero temperature gradient normal to the boundary line is assumed.

The following boundary conditions are then applied:

a) at any cylinder surface

$$U = 0\,, \quad V = 0\,, \quad T = 1 \tag{4}$$

b) at boundary line A–B

$$\frac{\partial U}{\partial X} = 0\,, \quad V = 0\,, \quad T = 0 \text{ if } U \geq 0 \text{ or } \frac{\partial T}{\partial X} = 0 \text{ if } U < 0 \tag{5}$$

c) at boundary line B–C

$$U = 0\,, \quad \frac{\partial V}{\partial Y} = 0\,, \quad T = 0 \text{ if } V < 0 \text{ or } \frac{\partial T}{\partial Y} = 0 \text{ if } V \geq 0 \tag{6}$$

d) at boundary line C–D

$$\frac{\partial U}{\partial X} = 0\,, \quad V = 0\,, \quad T = 0 \text{ if } U < 0 \text{ or } \frac{\partial T}{\partial X} = 0 \text{ if } U \geq 0 \tag{7}$$

e) at boundary line A–D

$$U = 0\,, \quad \frac{\partial V}{\partial Y} = 0\,, \quad T = 0 \text{ if } V > 0 \text{ or } \frac{\partial T}{\partial Y} = 0 \text{ if } V \leq 0 \tag{8}$$

As far as the intersections between polar and Cartesian grids are concerned, the value of each of the dependent variables at any false node of one of the two neighbouring grids is obtained by a linear interpolation of the values of the same variable at the four surrounding real nodes of the other grid.

Solution algorithm

The set of equations (1)–(3) with the b.c.'s (4)–(8) is solved through a control-volume formulation of the finite-difference method. The pressure-velocity coupling is handled by the SIMPLE–C algorithm by Van Doormaal and Raithby [5]. The advection fluxes across the surfaces of the control volumes are evaluated by the QUICK discretization scheme by Leonard [6].

Fine uniform mesh-spacings are used for the discretization of both the polar grid regions and the Cartesian grid region.

Starting from first-approximation fields of the dependent variables, the discretized governing equations are solved iteratively through a line-by-line application of the Thomas algorithm, enforcing under-relaxation to ensure convergence.

Table 1 - Comparison of the present results with the benchmark solutions of Saitoh et al.

Ra		$Nu_0(\theta)$							Nu_0
		θ = 0°	30°	60°	90°	120°	150°	180°	
10^3	Present	3.789	3.755	3.640	3.376	2.841	1.958	1.210	3.023
	Saitoh *et al.* [7]	3.813	3.772	3.640	3.374	2.866	1.975	1.218	3.024
10^4	Present	5.986	5.931	5.756	5.406	4.716	3.293	1.532	4.819
	Saitoh *et al.* [7]	5.995	5.935	5.750	5.410	4.764	3.308	1.534	4.826
10^5	Present	9.694	9.595	9.297	8.749	7.871	5.848	1.989	7.886
	Saitoh *et al.* [7]	9.675	9.577	9.278	8.765	7.946	5.891	1.987	7.898

The solution is considered to be converged when the maximum absolute values of both the mass source and the percent changes of the dependent variables at any grid-node from iteration to iteration are smaller than prescribed values, i.e., 10^{-4} and 10^{-6}, respectively.

After convergence is attained, the local and average Nusselt numbers $Nu_i(\theta)$ and Nu_i for the i-th cylinder in the array are calculated:

$$Nu_i(\theta) = \frac{q_i D}{k(t_w - t_\infty)} = -\left.\frac{\partial T}{\partial r}\right|_{r=0.5} \tag{9}$$

$$Nu_i = \frac{Q_i}{\pi k(t_w - t_\infty)} = -\frac{1}{2\pi}\int_0^{2\pi}\left.\frac{\partial T}{\partial r}\right|_{r=0.5} d\theta \tag{10}$$

where q is the heat flux and Q is the heat transfer rate. The temperature gradients at any cylinder surface are evaluated by assuming a second-order temperature profile among each wall-node and the next two fluid-nodes. The integrals are approximated by the trapezoid rule. The average Nusselt number of the whole assembly Nu is then obtained as the arithmetic mean value of the average Nusselt numbers Nu_i of the individual cylinders.

Validation of the numerical procedure

Tests on the dependence of the results obtained on the mesh-spacing of both the polar and the Cartesian discretization grids, as well as on the thickness of the polar grid regions, and on the extent of the whole computational domain, have been performed for several combinations of values of N, φ and Ra. In particular, the optimal grid-size values, and the optimal positions of the polar/Cartesian interfaces and the outer pseudo-boundary lines used for computations (representing a good compromise between solution accuracy and computational time), are such that further grid refinements or boundary displacements do not yield for noticeable modifications neither in the heat transfer rates nor in the flow field, that is, the percent changes of $Nu_i(\theta)$ and Nu_i, and the percent changes of the maximum value of the tangential velocity components at θ = (90°+φ) and θ = (270°+φ) for any cylinder, are smaller than prescribed accuracy values, i.e., 1% and 2%, respectively. Typical features of the integration domain may be summarized as follows: (a) the number of nodal points (r×θ) of the polar grids lies in the range between 45×72 and 180×108, (b) the thickness of the polar grid regions varies between one-fifth and one-half of the cylinder-diameter, and (c) the extent of the whole integration domain ranges between 4 and 10 diameters upwards, between 2 and 4 diameters downwards, and between 3 and 6 diameters sidewards, depending on the Rayleigh number, the number of cylinders, and the tilting angle.

As far as the validation of both the numerical code and the meshing procedure is specifically concerned, a comparison between the local and average Nusselt numbers $Nu_0(\theta)$ and Nu_0 obtained for a single cylinder at several Rayleigh numbers and the corresponding benchmark results by Saitoh et al. [7], is reported in Table 1. Moreover, in order to test the reliability of the composite polar/Cartesian grid system used, a comparison between the overall results obtained for a two-cylinder array and the corresponding experimental data by Sparrow and Boessneck [2], are reported in Table 2. Many more details on the code validation are available in reference [4].

Table 2 - Comparison with the experimental data of Sparrow et al.

Ra	S/D	φ	Nu/Nu_0	
			Sparrow and Boessneck [2]	Present
6×10^4	2.0	0°	0.84	0.86
	2.1	14°	0.93	0.94
	2.2	27°	1.04	1.03
	5.0	0°	1.13	1.16
	5.1	11°	1.04	1.04
	5.4	22°	1.03	1.04
1×10^5	2.0	0°	0.85	0.88
	2.1	14°	0.93	0.96
	2.2	27°	1.03	1.04
	5.0	0°	1.18	1.18
	5.1	11°	1.04	1.04
	5.4	22°	1.03	1.04
2×10^5	2.0	0°	0.87	0.90
	2.1	14°	0.94	0.97
	2.2	27°	1.03	1.04
	5.0	0°	1.21	1.20
	5.1	11°	1.04	1.05
	5.4	22°	1.03	1.04

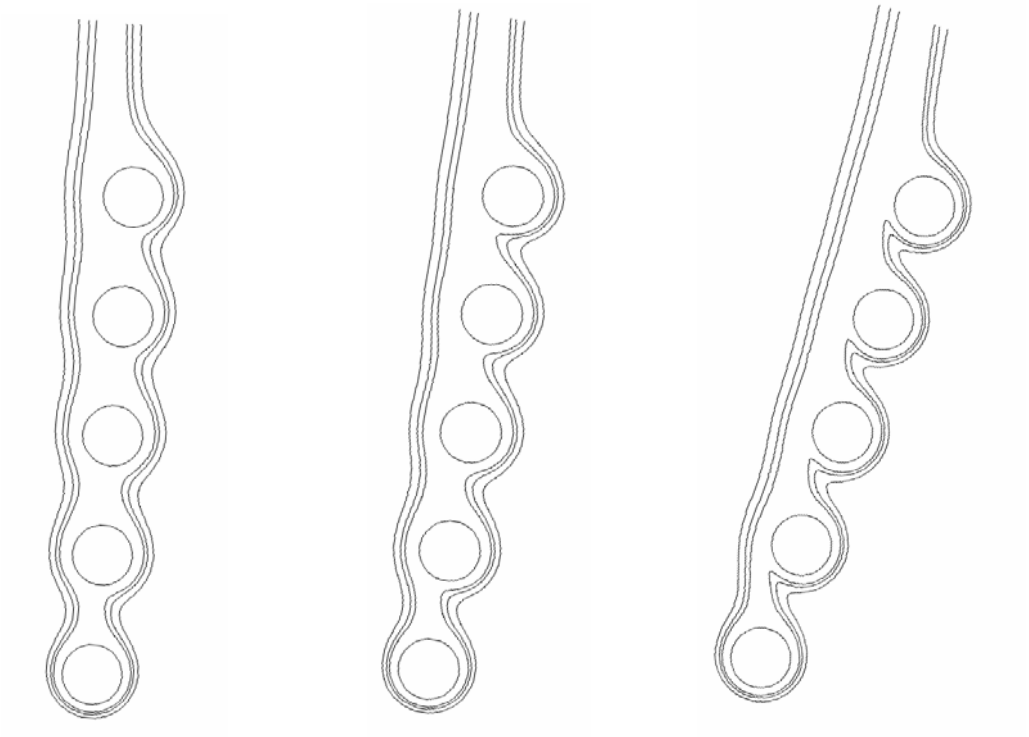

(a) φ = 5° (b) φ = 10° (c) φ = 20°

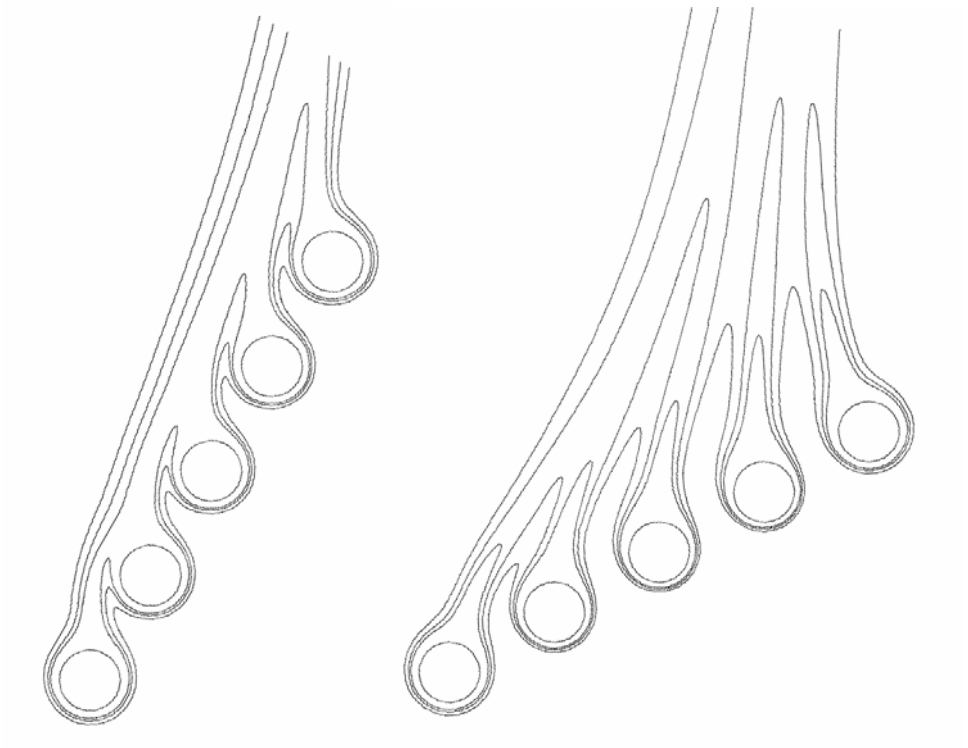

(d) φ = 30° (e) φ = 60°

Figure 2 – Isotherm contour plots for N = 5, Ra = 10^4 and different tilting angles

RESULTS AND DISCUSSION

Numerical simulations are performed for Pr = 0.71, which corresponds to air, and for different values of (a) the Rayleigh number Ra in the range between 10^2 and 10^6, (b) the tilting angle of the array φ with respect to the gravity vector, in the range between 0° and 90°, which correspond to the vertical and horizontal configurations, respectively, and (c) the number of cylinders in the range between 3 and 7. A dimensionless center-to-center separation distance S/D = 2 is assumed throughout the simulations, as such close cylinder-spacing is deemed of more interest under the point of view of the engineering applications.

Effects of the tilting angle

Isotherm contour plots for a 5-cylinder assembly at Ra = 10^4 are reported in Figs. 2(a)–2(e) for tilting angles φ = 5°, 10°, 15°, 30°, and 60°, respectively. It may be seen that the mutual interactions among the cylinders give rise to a "suction effect" which increases with increasing the tilting angle of the array. Owing to the consequent airflow through the gaps between the cylinders, the plume generated by any cylinder is more or less deflected, which implies that the lower and upper stagnation points of any cylinder rotate with respect to the vertical plane passing through the cylinder-axis. This is, e.g., shown in Fig. 3, where the polar distributions of the local Nusselt number $Nu_i(\theta)$ for any individual cylinder (numbered from N_1 to N_N from the bottom to the top of the tube-array) are shown for N = 5, Ra = 10^4, and φ = 60°. It may be noticed that the rear stagnation point of the bottom cylinder is rotated clockwise by an angle of 15°, whilst that of the top cylinder is rotated anticlockwise by an angle of nearly 30°.

The effects of the tilting angle φ on the heat transfer rate from the i-th cylinder of a 5-cylinder array at, e.g., Ra = 10^4, are shown in Fig. 4, where the results are expressed in terms of the ratio Nu_i/Nu_0 in order to highlight in what measure the convective interactions among the cylinders either enhance or degrade the heat transfer performance of any cylinder with respect to that of a single cylinder at same Rayleigh number.

It may be observed that when the tube-array is set vertically, the heat transfer performance of the first cylinder is substantially identical to that for a single cylinder. In contrast, the amount of heat exchanged by any downstream cylinder decreases with elevation along the array. In fact, since the buoyant airstream which washes the downstream cylinders gets warmer whilst moving upwards, the temperature difference between the cylinder surface and the adjacent fluid becomes progressively smaller. However, since the buoyant airstream becomes faster as it moves upwards, such "forced convection" effect tends to mitigate the negative temperature-effect cited above, which implies that the degree of degradation of the heat transfer rate with elevation is progressively less pronounced.

As the tube-array is tilted of an angle φ with respect to the gravity vector, two positive situations occur, which enhance the heat transfer performance of the cylinders. First, the negative washing-effect discussed above decreases progressively with increasing φ, up to vanishing when the plume generated by any cylinder does not impinge anymore upon the cylinder located downstream in the array. Secondly, a sort of "chimney effect" arises between the cylinders, which drives an increased mass flow rate of fresh air between them; the more the tube-array is inclined, the higher is the through-flow airstream between the cylinders. Accordingly, also the heat transfer performance of the whole assembly relative to that of a single cylinder Nu/Nu_0 increases with φ, as shown in Fig. 5 for a 5-cylinder array at different Rayleigh numbers.

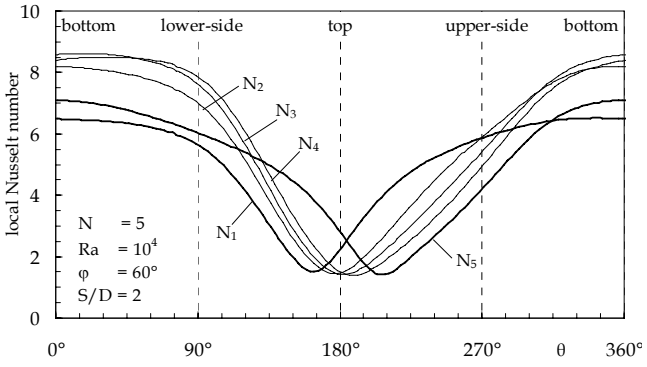

Figure 3 –$Nu_i(\theta)$ vs. θ for N = 5, Ra = 10^4 and φ = 60°

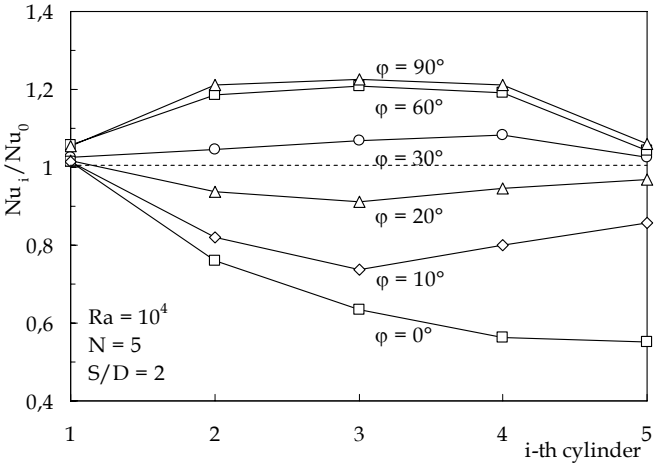

Figure 4 –Nu_i/Nu_0 for N = 5, Ra = 10^4 and different values of φ

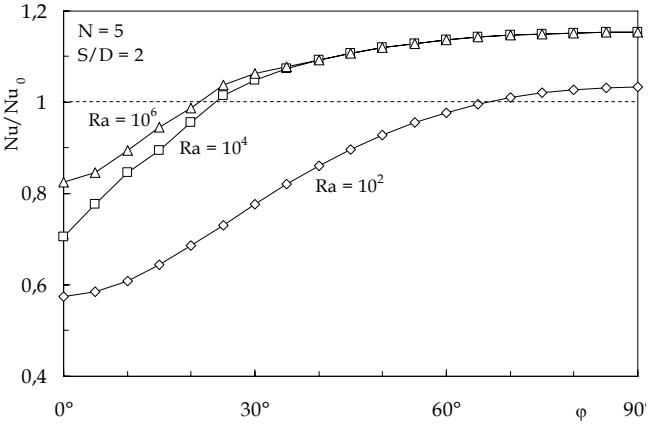

Figure 5 –Nu/Nu_0 vs. φ for N = 5 and different values of Ra

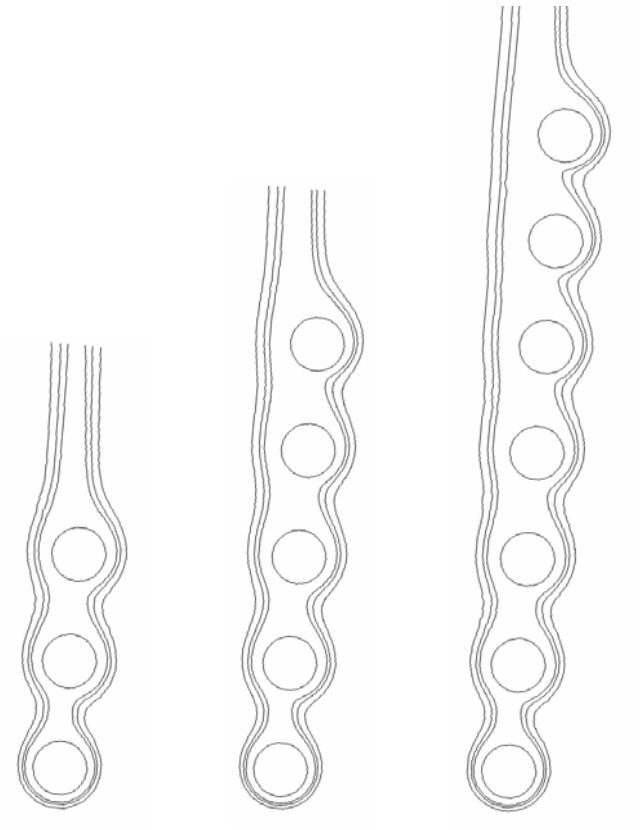

(a) N = 3 (b) N = 5 (c) N = 7

Figure 6 – Isotherm contour plots for φ = 5°, Ra = 10^4 and N = 3, 5, and 7

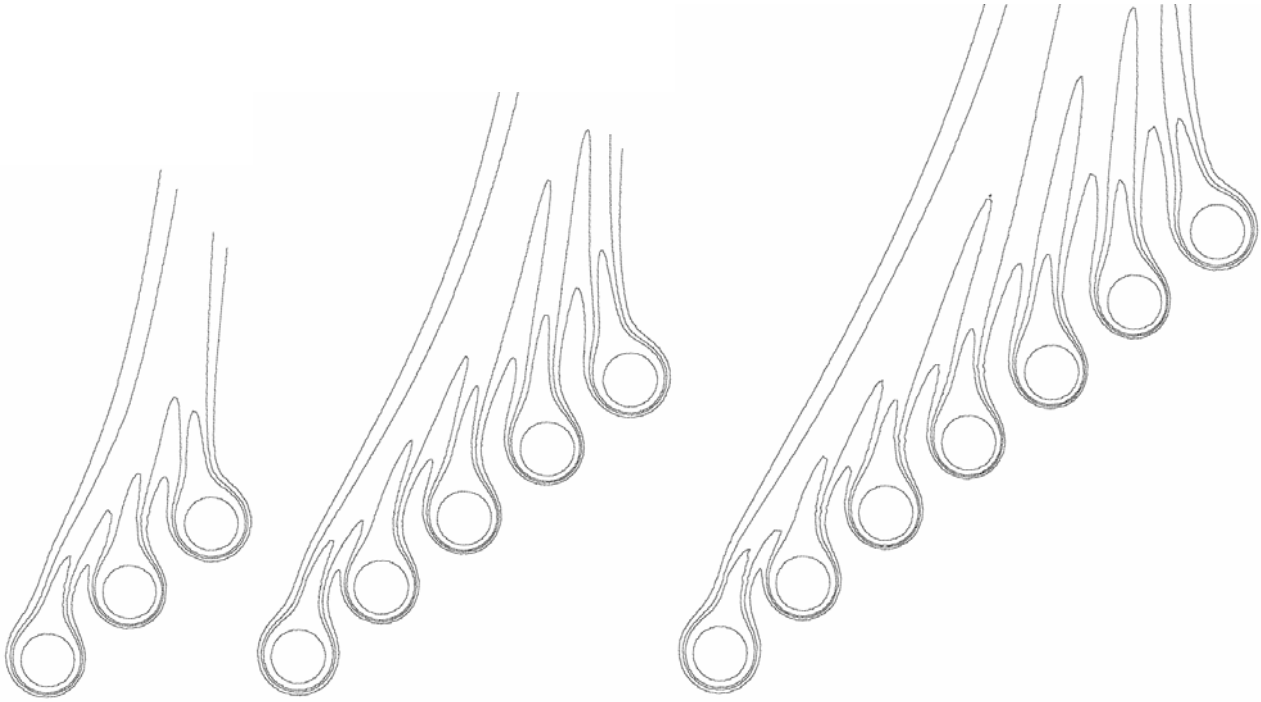

(a) N = 3 (b) N = 5 (c) N = 7

Figure 7 – Isotherm contour plots for φ = 50°, Ra = 10^4 and N = 3, 5, and 7

Effects of the number of cylinders

Isotherm contour plots are depicted in Figs. 6(a)–(c) and in Figs. 7(a)–(c) for Ra = 10^4, N = 3, 5, and 7, and φ = 5° and 50°.

The effects of the number of cylinders on the relative heat transfer performance of the whole tube-array are pointed out in Fig. 8, where the distributions of Nu/Nu_0 vs. φ are reported for Ra = 10^4 and different values of N. It may be noticed that the relative heat transfer performance of the array either decreases or increases with increasing N, according as φ is small or large, i.e., φ is smaller than nearly 10° or larger than 15–20°. In fact, for quasi-vertical configurations, the amount of heat exchanged by any cylinder is smaller than that exchanged by the preceding cylinder, thus implying that any element added to the array worsens the whole heat transfer performance. In contrast, for more inclined configurations, in which the mutual convective interactions between the cylinders are governed exclusively by the chimney effect, the higher is the number of cylinders, the more pronounced is the chimney effect generated by the array.

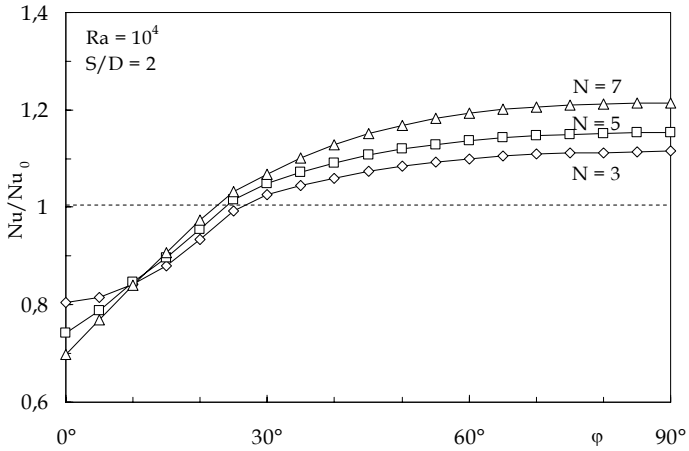

Figure 8 – Nu/Nu_0 vs. φ for Ra = 10^4 and different values of N

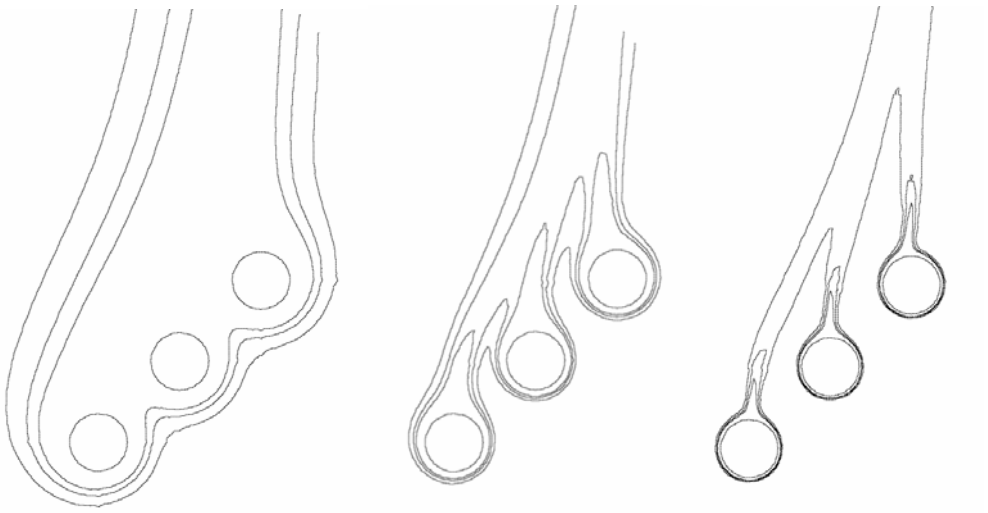

(a) Ra = 10^2 (b) Ra = 10^4 (c) Ra = 10^6

Figure 9 – Isotherm contour plots for φ = 45°, N = 3 and Ra = 10^2, 10^4, and 10^6

Effects of the Rayleigh number

Isotherm contour plots for a 3-cylinder array are depicted in Figs. 9(a)–(c) for φ=45° and Ra=10^2, 10^4 and 10^6, respectively.

It seems worth pointing out that, for small values of Ra, the thermal behavior of the whole tube-array resembles that of an inclined plate, whereas, for larger values of Ra, the plumes spawned by the cylinders tend to retain their individuality.

Moreover, as expected, it is evident how the increase in Rayleigh number brings to an increase in the chimney effect, and then in the amount of heat exchanged, as shown in Fig. 10, where the distributions of Nu vs. Ra for N = 3 are reported for different values of φ.

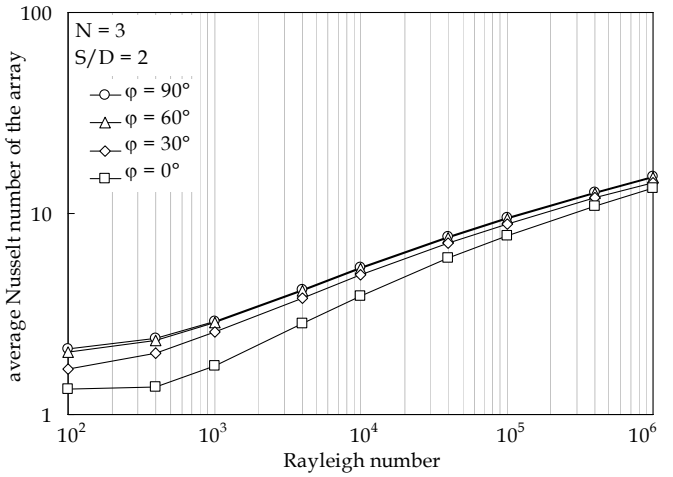

Figure 10 –Nu vs. Ra for N = 3 and different values of φ

CONCLUSIONS

Free convection in air from a inclined tube-arrays consisting of 3–7 circular cylinders equally-spaced at a center-to-center separation distance of 2 cylinder-diameters, has been studied

numerically for tilting angles from 0° to 90° (corresponding to the vertical and horizontal settings, respectively), and Rayleigh numbers in the range between 10^2 and 10^6.

Among the several results obtained, it has been found that the heat transfer performance of the whole tube-array increases with increasing both the Rayleigh number and the tilting angle, and as the number of cylinders in the array either decreases at very small tilting angles, i.e., for angles φ smaller than nearly 10°, or increases at inclination angles larger than about 15–20°.

NOMENCLATURE

D diameter of the cylinders
g gravity vector
g gravitational acceleration
k thermal conductivity of the fluid
N number of cylinders
Nu average Nusselt number of the whole array
Nu_i average Nusselt number of the i-th cylinder
$Nu_i(\theta)$ local Nusselt number of the i-th cylinder
Nu_0 average Nusselt number of the single cylinder
p dimensionless pressure
Pr Prandtl number = ν/α
Q heat transfer rate
q heat flux
r dimensionless radial coordinate normalized with D
Ra Rayleigh number based on the cylinder diameter = $= g\beta(t_w - t_\infty)D^3/\alpha\nu$
S centre-to-centre cylinder spacing
T dimensionless temperature
t temperature
U dimensionless radial or X-wise velocity component
V dimensionless velocity vector
V dimensionless tangential or Y-wise velocity component
X, Y dimensionless Cartesian coordinates normalized with D

Greek symbols

α thermal diffusivity of the fluid
β coefficient of volumetric thermal expansion of the fluid
φ tilting angle of the array with respect to gravity
ν kinematic viscosity of the fluid
θ dimensionless polar coordinate
ρ density of the fluid

Subscripts

i i-th cylinder in the array
w cylinder surface
∞ undisturbed fluid

REFERENCES

[1] J. Lieberman and B. Gebhart, Interaction in natural convection from an array of heated elements, experimental, Int. J. Heat Mass Transfer 12 (1969) 1385-1396.

[2] E. M. Sparrow and D. S. Boessneck, Effect of traverse misalignment on natural convection from a pair of parallel, vertically stacked, horizontal cylinders, J. Heat Transfer 105 (1983) 241-247.

[3] B.E. Launder and T. H. Massey, The numerical prediction of viscous flow and heat transfer in tube banks, J. Heat Transfer 100 (1978) 565-571.

[4] M. Corcione, Correlating equations for free convection heat transfer from horizontal isothermal cylinders set in a vertical array, Int. J. Heat Mass Transfer 48 (2005) 3660-3673.

[5] J. P. Van Doormaal and G. D. Raithby, Enhancements of the simple method for predicting incompressible fluid flows, Numer. Heat Transfer 11 (1984) 147-163.

[6] B. P. Leonard, A stable and accurate convective modelling procedure based on quadratic upstream interpolation, Comp. Meth. in Appl. Mech. Engng. 19 (1979) 59-78.

[7] T. Saitoh, T. Sajiki and K. Maruhara, Benchmark solutions to natural convection heat transfer problem around a horizontal circular cylinder, Int. J. Heat Mass Transfer 36 (1993) 1251-1259.